160 Transactions of the Korean Society of Mechanical Engineers, Vol. 6, No. 2, pp.160~168, 1982.

<Original>

An Expermental and Numerical Study of Natural Convection in the Annuli between Horizontal Confocal Elliptic Cylinders†

Jae Heon Lee* and Taik Sik Lee**

(Received November 14, 1981)

水平同心 楕圓사이의 環狀空間에서의 自然對流에 關한 數値 및 實驗的 硏究

李 在 憲 · 李 澤 植

抄 錄

水平으로 놓여진 2개의 同心楕圓 사이의 環狀空間에서의 自然對流現象이 數値計算 및 實驗的으로 硏究 되었다.

數値的 硏究는 定常 2次元 層流流動領域에서 수행되었으며 流線 및 等溫線이 求하여 졌다. 또한 특수한 경우로서 水平同心圓 사이의 環狀空間에 關한 旣存硏究와 比較하여 좋은 一致를 보았다.

實驗的 硏究에서는 3개의 實驗모델을 製作하였으며 마하젠더 干涉計에 의한 干涉寫眞으로 부터 等溫線 分布를 얻었으며 아울러 流動에 관한 정보도 얻을 수 있었다.

實驗과 數値計算結果는 상당히 좋은 一致를 보였으며 旣存 同心圓環狀空間에 偏心率이 추가된 理論展開 및 數値計算方法의 適合性을 알 수 있었고 이로서 環狀空間에서의 自然對流에 關한 硏究를 擴張시켰다.

Nomenclature

a : Focal length (m);
A : Characteristic length (m);
F : Body force (kg·m/s²);
g : Acceleration of gravity (m/s²);
G : Gap ratio,
=(max. gap width+min. gap width)/(length of major axis of inner cylinder+that of minor axis);
h : Metric coefficient (m);
H : Dimensionless metric coefficient;
Nu : Nusselt number;
P : Pressure (Pa);
Pr : Prandtl number;
R : Dimensionless radius,
$=(u-u_i)/(u_o-u_i)$;
Ra : Rayleigh number;
T : Temperature (°C);
$\triangle T$: Difference between surface temperature,
$=(T_i-T_o)$ (°C);
u : Radial independent variable;
U : Dimensionless radial velocity;

† Presented at Autumn Conference of Korean Society of Mechanical Engineers, 1980

* Member, Han-Yang Univ.
** Member, Seoul National Univ.

v : Angular independent variable;
V : Dimensionless angular velocity;
V_u : Radial velocity (m/s);
V_v : Angular velocity (m/s);
W : Dimensionless vorticity;

Greek symbols

α : Thermal diffusivity (m^2/s);
β : Thermal expansion coefficient (1/°C);
ε : Eccentricity;
θ : Angle, in equation (9);
Θ : Dimensionless temperature;
ν : Kinematic viscosity (m^2/s);
ρ : Density (kg/m^3);
ϕ : Stream function (m^2/s);
Ψ : Dimensionless stream function;

Subscripts

i : Refers to inner cyilnder;
L : Max. gap width, refers to characteristic length on Rayleigh number;
o : Refers to outer cylinder;

1. Introduction

In recent years, natural convection in enclosed space has received an increasing attention both theoretically and experimentally. However it is not well understood on the behavior of natural convectionin horizontal annulus expect between circular cylinders. It will be, however, necessary to obtain the information about natural convection in horizontal annulus between non-circular cylinders.

This work is concerned with a natural convection in horizontal annulus between confocal elliptic cylinders, which is the typical example of variable curvature and is possible to adopt the orthogonal elliptic cylindrical coordinate system. Since the analysis of elliptic cross section has a generality which can involve the case of circular section, and since the flow around the inner cylinder resembles that around a single horizontal cylinder when the ratio of outer cylinder to inner cylinder is very large, the individual analysis of the natural convection from a single horizontal circular cylinder or a single horizontal elliptic cylinder or between two horizontal circular cylinders becomes unnecessary. This method has the wider application than the previous one does.

Kuehn[1] extended the information about velocity and temperature distribution and local heat transfer coefficient with an excellent review in the annulus between horizontal concentric circular cylinders.

In this work, using governing equation which contains another nonlinear parameter, eccentricity, in addition to the equation of horizontal annular cross-sections, the natural convection between horizontal confocal elliptic cylinders has been studied near the Prandtl number 0.7. In order to verify the generality of this method, the result were compared with those of annulus between horizontal concentric circular cylinders, and with experiments which were performed by Mach-Zehnder interferometer.

2. Theoretical Study

2.1. Analysis

We consider a steady laminar two-dimensional natural convection of a fluid enclosed in between two confocal elliptic cylinders whose common axis is horizontal. The temperature of each cylinder is uniform. A vertical plane

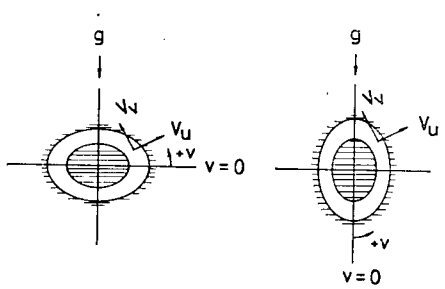

Fig. 1 Coordinate system.

through the centre of the system divides the flow into two symmetric halves, so that only one side needs to be studied. The Boussinesq approximation of the constant fluid properties is used.

According to the posture of annulus, there can be two positions as shown in Fig. 1. So we designate the left as lying position and the right as standing position. And u is a radial coordinate while v is an angular coordinate measured counterclockwise from lower vertical symmetric line which designates zero and $-\pi/2$ at standing and lying position respectively. The governing differential equations for the problem described above result in the following elliptic coupled, time-independent equations in elliptic cylindrical coordinates;

$$\frac{\partial V_u}{\partial u}+\frac{\partial V_v}{\partial v}+\frac{a^2}{2h^2}(\sinh 2u\cdot V_u+\sin 2v\cdot V_v)=0 \tag{1}$$

$$\rho\left[\frac{V_u}{h}\frac{\partial V_u}{\partial u}+\frac{V_v}{h}\frac{\partial V_v}{\partial v}-\frac{a^2\sinh 2u}{2h^3}V_u^2+\frac{a^2\sin 2v}{2h^3}V_uV_v\right]=-\frac{1}{h}\frac{\partial P}{\partial u}+\frac{\mu}{h^2}\left[\frac{\partial^2 V_u}{\partial u^2}+\frac{\partial^2 V_u}{\partial v^2}+\frac{\partial V_v}{\partial u}\cdot\frac{a^2\sin 2v}{h^2}-\frac{\partial V_v}{\partial v}\frac{a^2\sinh 2u}{h^2}-V_u\cdot\frac{a^2(\cos 2v+\cosh 2u)}{2h^2}\right]+F_u \tag{2}$$

$$\rho\left[\frac{V_u}{h}\frac{\partial V_v}{\partial u}+\frac{V_v}{h}\frac{\partial V_v}{\partial v}-\frac{a^2\sin 2v}{2h^3}V_v^2+\frac{a^2\sinh 2u}{2h^3}V_uV_v\right]=-\frac{1}{h}\frac{\partial P}{\partial v}+\frac{\mu}{h^2}\left[\frac{\partial^2 V_v}{\partial u^2}+\frac{\partial^2 V_v}{\partial v^2}+\frac{\partial V_u}{\partial v}\cdot\frac{a^2\sinh 2u}{h^2}-\frac{\partial V_u}{\partial u}\frac{a^2\sin 2v}{h^2}-V_v\frac{a^2(\cos 2v+\cosh 2u)}{2h^2}\right]+F_v \tag{3}$$

$$V_u\frac{\partial T}{\partial u}+V_v\frac{\partial T}{\partial v}=\frac{\alpha}{h}\left(\frac{\partial^2 T}{\partial u^2}+\frac{\partial^2 T}{\partial v^2}\right) \tag{4}$$

The body force terms can be written as following:

for lying position

$$F_u=-\rho g\beta\,\triangle T\cos\theta, \tag{5}$$

$$F_v=\rho g\beta\,\triangle T\sin\theta, \tag{6}$$

for standing position

$$F_u=\rho g\beta\,\triangle T\sin\theta, \tag{7}$$

$$F_v=\rho g\beta\,\triangle T\cos\theta, \tag{8}$$

where θ is an angle between gravitational acceleration and tangential line or normal line on the surface of inner cylinder;

$$\theta=\arctan\frac{\cosh u\sin v}{\sinh u\cos v} \tag{9}$$

Use of the stream function φ instead of the velocity terms automatically statisfies the continuity equation by setting

$$V_u=\frac{1}{h}\frac{\partial\varphi}{\partial v},\quad V_v=-\frac{1}{h}\frac{\partial\varphi}{\partial u} \tag{10}$$

The above equations are made dimensionless by setting

$$H=\frac{h}{A},\quad U=\frac{A}{\alpha}\frac{1}{h}\frac{\partial\varphi}{\partial v},\quad V=-\frac{A}{\alpha}\frac{1}{h}\frac{\partial\varphi}{\partial u},\quad \Theta=\frac{T-T_o}{\triangle T},\quad \Psi=\frac{\varphi}{\alpha},\quad Pr=\frac{\nu}{\alpha},\quad Ra=\frac{g\beta\triangle TA^3}{\alpha\nu} \tag{11}$$

where A is a characteristic length. The geometry of elliptic annulus depends on focal lengths and eccentricities of the two ellipses. It is, therefore, difficult to describe the whole phenomena with only one characteristic length among many related lengths. It may be chosen the maximum gap width of annulus, length of long axis, or perimeter of the inner ellipse as the characteristic length according to the field of interest. In this paper we use Ra_L only whose characteristic length is maximum gap width. The corresponding value of the Rayleigh number is based on properties evaluated at the arithmetic mean temperature, $(T_o+T_i)/2$.

For convenience, we define dimensionless vorticity as

$$W=-\nabla^2\Psi. \tag{12}$$

Therefore at lying posistion, the equations to

be solved are

$$\nabla^2 \Psi = -W \tag{13}$$

$$\nabla^2 W = \frac{1}{H} Ra \left[\xi \left(\frac{\Theta \sin\theta \sin 2v}{2} - \frac{\Theta \cos\theta \sinh 2u}{2} \right) + \frac{\partial \Theta}{\partial v} \sin\theta - \frac{\partial \Theta}{\partial u} \cos\theta + \frac{1}{H} \frac{1}{Pr} \left(U \frac{\partial W}{\partial u} + V \frac{\partial W}{\partial v} \right) \right], \tag{14}$$

$$\nabla^2 \Theta = \frac{1}{H} \left(U \frac{\partial \Theta}{\partial u} + V \frac{\partial \Theta}{\partial v} \right). \tag{15}$$

At standing position, equation (16) must be used instead of equation (14);

$$\nabla^2 W = -\frac{1}{H} Ra \left[\xi \left(\frac{\Theta \cos\theta \sin 2v}{2} - \frac{\Theta \sin\theta \sinh 2u}{2} \right) + \frac{\partial \Theta}{\partial v} \cos\theta + \frac{\partial \Theta}{\partial u} \sin\theta \right] + \frac{1}{H} \frac{1}{Pr} \left(U \frac{\partial W}{\partial u} + V \frac{\partial W}{\partial v} \right), \tag{16}$$

where

$$\xi = \frac{1}{\sinh^2 u + \sin^2 v} - \frac{1}{\sinh^2 u \cos^2 v + \cosh^2 u \sin^2 v},$$

$$\nabla^2 = \frac{1}{H^2} \left(\frac{\partial^2}{\partial u^2} + \frac{\partial^2}{\partial v^2} \right). \tag{17}$$

The boundary conditions imposed are two solid walls and two vertical lines of symmetry. The dimensionless temperature is equal to unity on the inner cylinder and zero on the outer cylinder. The angular derivatives of the temperature vanish at the lines of symmetry. Since no flow enters or escapes from the walls as along as the lines of symmetry, the stream function is set equal to zero on all the boundaries. The vorticity on the symmetry lines is set equal to zero because of the odd function across the symmetry lines. The angular derivative of vorticity term vanishes on the wall due to the zero tangential velocities along the wall. Therefore the boundary conditions become

$$\left.\begin{array}{l} \text{for lying,} \quad v = \pm\dfrac{\pi}{2} \\ \text{for standing,} \quad v = 0,\ \pi \end{array}\right\} : \Psi = V = W = \frac{\partial \Theta}{\partial v} = \frac{\partial U}{\partial v} = 0, \tag{18}$$

$$u = u_i \quad : \Psi = U = V = \frac{\partial^2 \Psi}{\partial v^2} = 0, \ \Theta = 1 \tag{19}$$

$$u = u_o \quad : \Psi = U = V = \frac{\partial^2 \Psi}{\partial v^2} = 0, \ \Theta = 0 \tag{20}$$

Equations (13) through (16) with boundary conditions were converted from differential equations to finite difference equations. These equations were programmed for solution using a successive over relaxation procedure. The whole space was subdivided into 16×19, 16×37, 32×19 or 24×25 according to the geometry of annulus. The calculations were performed on the FACOM 230-28S COMPUTER.

2.2. Result and Discussion

In order to verify the validity of this analysis, conditions of previous study of Kuehn & Goldstein[2] has been selected in case of the annulus between concentric circular cylinders. We calculated the natural convection at both positions by forming the almost perfect concentric circular annulus for which the length

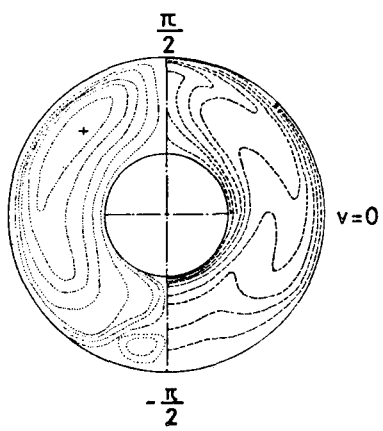

Fig. 2 Streamlines and isotherms for $Ra_L = 5.0 \times 10^4$, $Pr = 0.7$, $a = 1.77$ mm, $\varepsilon_i = 0.099$, $\varepsilon_o = 0.038$.

of minor axis was above 99.5% of that of major axis for inner cylinder, because the perfect concentric circular annulus must lie between lying and standing positions.

When the gap ratio G was 0.8 and Ra_L was 5×10^4, the results of both positions were qualitatively the same, showing a difference less than 0.05% from each other. Figure 2 shows resulting isotherms and streamlines. For the most part of annulus, our result agrees with Kuehn & Goldstein's result in respect of average heat transfer rate, temperature distribution and velocity field of flow. But some discrepancy can be found at the lower portion. In our result, there is a weak steady counter-rotating-flow pattern in the lower portion of the annulus, but in Kuhen & Goldstein's result there is no clear expression of that. And because of this flow pattern, the position of maximum heat transfer coefficient of inner cylinder is not exactly at the bottom but about $\pi/4$ in angular direction above from the bottom. This kind of flow pattern could also be observed in the result of Bishop et al.[3], when the type of flow was kidney-shaped eddy pattern. In the lower portion of the annulus, this pattern is presumably caused by the strong eddy in the upper portion of the annulus when the the centre of eddy, i.e., the position of maximum stream function moves upwards far from the middle of annulus.

As an example of elliptic annulus, we chose a condition with $a=2.11$ mm, $\varepsilon_i=0.600$, $\varepsilon_o=0.475$ and $Pr=0.708$. At $Ra_L=3.71\times10^3$ with above condition, the streamlines and isotherms are shown in Fig. 3 and Fig. 4 according to positions respectively. The isotherms move upward like eccentric ellipses at both positions, this kind of moving was also reported in the results of circular annulus previously. And the position of maximum stream function moves

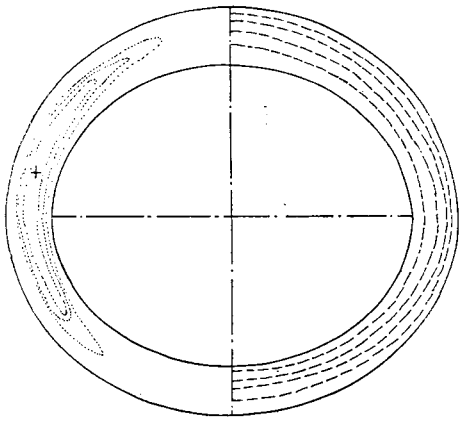

Fig. 3 Streamlines and isotherms at lying position for $Ra_L=3.71\times10^4$, $Pr=0.708$, $a=2.11$ mm, $\varepsilon_i=0.600$, $\varepsilon_o=0.475$.

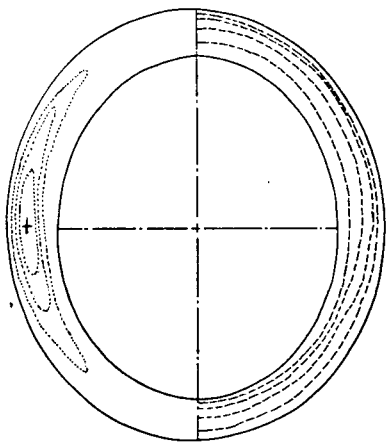

Fig. 4 Streamlines and isotherms at standing position for $Ra_L=3.71\times10^3$, $Pr=0.708$, $a=2.11$ mm, $\varepsilon_i=0.600$, $\varepsilon_o=0.475$.

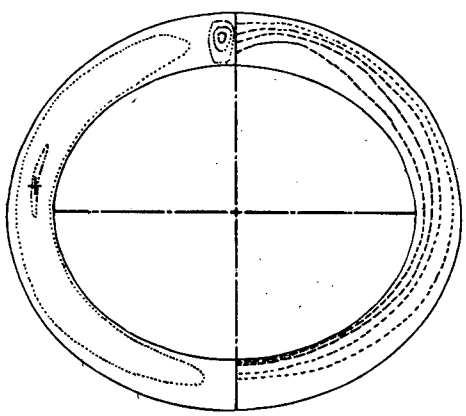

Fig. 5 Streamlines and isotherms at lying position for $Ra_L=9.00\times10^3$, $Pr=0.708$, $a=2.11$ mm, $\varepsilon_i=0.600$, $\varepsilon_o=0.475$.

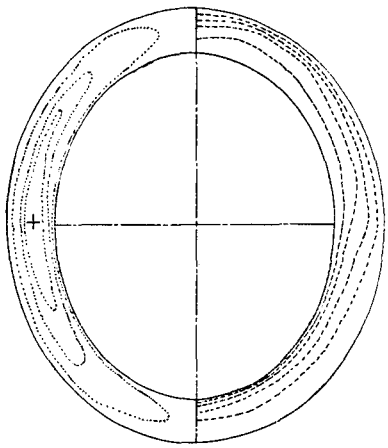

Fig. 6 Streamlines and isotherms at standing position for $Ra_L=9.00\times10^3$, $Pr=0.708$, $a=2.11$ mm, $\varepsilon_i=0.600$, $\varepsilon_o=0.475$.

upwards at lying position while this position remains on the centre of the annulus at standing position. At $Ra_L=9.00\times10^3$, Figure 5 and 6 show the streamlines and isotherms. The "hump" pattern appears in the isetherms, and the counter-rotating flow pattern appears in the streamlines at upper portion of the annulus of the lying position. But at standing position, the isotherms move slightly more upwards than the case of $Ra_L=3.71\times10^3$ and there is a symptom of temperature inversion at the middle portion of the annulus. The differences which arise between the two positions as Rayleigh number increases are believed to be caused by the face that the flow in annulus is more affected by the posture of annulus as the effect of natural convection increases.

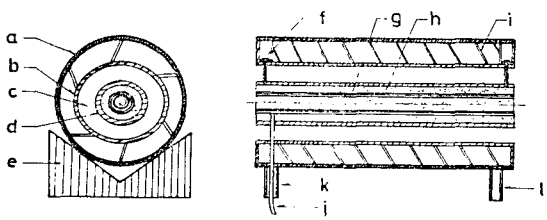

Fig. 7 Schematic diagram of horizontal elliptical annulus.
a: cooling water jacket
b: outer elliptic cylinder
c: test section
d: inner elliptic cylinder
e: V block type support
f: fixing screw
g: thermal conductor
h: heater
i: cooling water guide vane
j: power and thermocouple lines
k: cooling water outlet
l: cooling water inlet.

3. Experimental Study

3.1. Apparatus and Procedure

The natural convection apparatus, shown schematically in Fig. 7, consists of two concentric elliptical cylinders enclosed in a cooling water jacket. A single outer elliptic cylinder with $\varepsilon_0=0.400$ and $a=20$mm was used in conjunction with three inner elliptic cylinders of 0.688, 0.574 and 0.474 eccentricities. These provided values of 0.456, 0.257 and 0.104 for the gap ratio G.

All cylinders were 250 mm long and of 3 mm thick copper, which helped to maintain isothermality within 0.5°C. The inner cylinder was heated by means of a bare nichrome wire which was located within the cylinder. The felstone powder was filled in space. The water, which maintained the outer cylinder at a uniform temperature, was introduced at the base and withdrawn at the top through a guide vain in the water jacket. In order to check the isothermalities of the both cylinders, three-welded-thermocouples were embedded in each cylinder at distinct position angularly and axially. The assembled apparatus was mounted on V-block type supporter to allow rotation during adjusting the vertical symmetric line to gravity direction.

Using Mach-Zehnder interferometer whose mirror-diameter is 20cm, the isotherms were taken. Interferogram was recorded on 70mm Verichrome film. The test fluid was air at the

ambient temperature and the atmospheric pressure. Auxillary apparatus and evaluation technique of interferograms are described in reference (4) in detail.

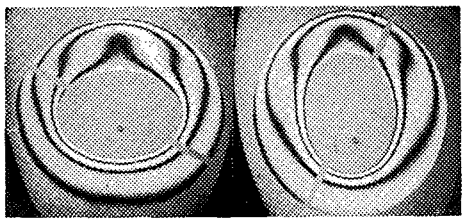

Fig. 8 Interferograms taken using air for $Ra_L=1.245\times10^4$, $Pr=0.710$, $a=20.0$ mm, $\varepsilon_i=0.688$, $\varepsilon_o=0.400$.

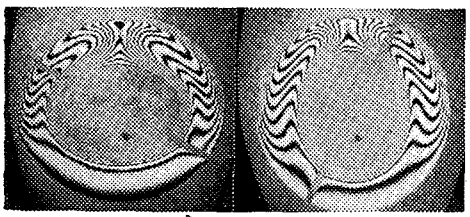

Fig. 9 Interferograms taken using air for $Ra_L=5.860\times10^4$, $Pr=0.705$, $a=20.0$ mm, $\varepsilon_i=0.688$, $\varepsilon_o=0.400$.

3.2. Experimental Results

For the gap ratio G of 0.456, experimented Ra_L are 0.716×10^4, 1.245×10^4, 3.793×10^4, 5.860×10^4 and 7.349×10^4. These conditions were achieved by varing temperature difference, ΔT, from 4°C to 81°C. Selected isotherms of both positions are shown in Fig. 8 and Fig. 9 whose Ra_L are 1.245×10^4 and 5.860×10^4 respectively. At both positions, a temperature inversion arises at $Ra_L=1.25\times10^4$ and flow region falls within steady two-dimensional boundary layer until Ra_L reaches 3.79×10^4. When $Ra_L=5.84\times10^4$ at lying position, the two-dimensional oscillations occurrs in isotherms of whole space except the lower portion of the annulus where the flow was practically stagnant, while at standing position this oscillation is observed within $\pm\pi/3$ from upper vertical symmetric line. The oscillatory region extended over the whole annulus at $Ra_L=7.35\times10^4$ on both positions. And its oscillatory frequency is about 1 Hz.

For the gap ratio G of 0.257, the range of Rayleigh number is from 2.34×10^3 to 2.20×10^4, with resulting temperature differences, ΔT, from 3°C to 61°C. The temperature inversion is observed with $Ra_L=6.51\times10^3$ and oscillation with $Ra_L=1.08\times10^4$ at both positison. The isotherms within $\pm\pi/6$ from the upper symmetric line are entangled at $Ra_L=1.81\times10^4$ of the lying position, as shown in Fig. 10. This phenomenon means that the flow region is transformed into three dimensional or turbu-

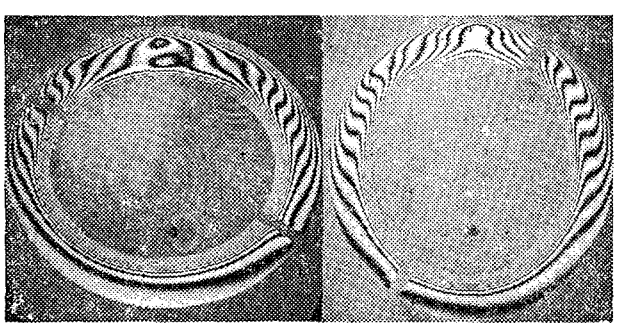

Fig. 10 Interferograms taken using air for $Ra_L=1.805\times10^4$, $Pr=0.706$, $a=20.0$mm, $\varepsilon_i=0.574$, $\varepsilon_o=0.400$.

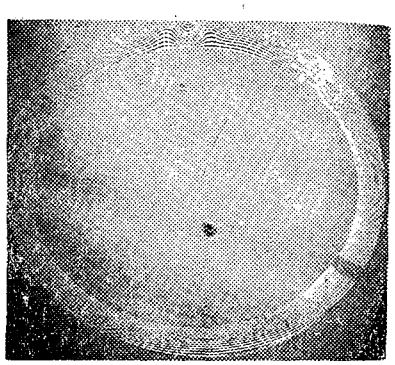

Fig. 11 Interferogram taken usnig air for $Ra_L=2.919\times10^3$, $Pr=0.704$, $a=20.0$ mm, $\varepsilon_i=0.474$, $\varepsilon_o=0.400$.

lent region. At $Ra_L=2.20\times10^4$ of the both positions, this kind of flow is observed within $\pm\pi/3$ from upper symmetric line.

For the smallest gap ratio G of 0.104, the range of Rayleigh number is from 0.44×10^3 to 3.38×10^3, with resulting temperature differences, ΔT, from 6°C to 92° C. At standing position over the experimented Rayleigh numbers, the isotherms whose pattern resembled an eccentric ellipses moves a little upward with increasing Rayleigh number. This indicates that there is little influence of convection in the whole space of annulus. In the region adjacent to the upper vertical symmetricl ine of the lying position, the isotherms begin to appear as a "hump" when the Ra_L reaches 2.11×10^3. This kind of isotherms' pattern appeared more distinctly from $Ra_L=2.92\times10^3$ as shown in Fig. 11. As discussed previously, when this pattern is shown at any experiment on natural convection using air, the flow direction can be considered to be downward on the vertical symmetric line of the concave isotherms.

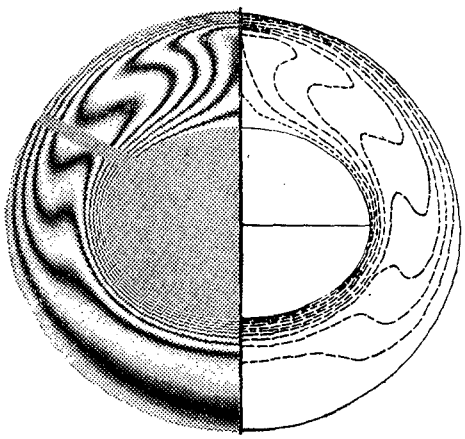

Fig. 12 Comparison between experimental and numerical isotherms at lying position for $Ra_L=3.795\times10^4$, $Pr=0.707$, $a=20.0$ mm. $\varepsilon_i=0.688$, $\varepsilon_o=0.499$.

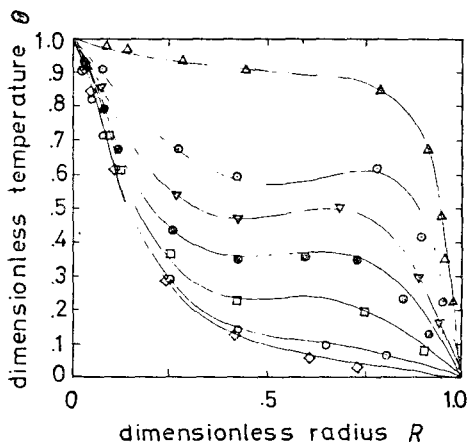

Fig. 13 Comparison between experimental and numerical temperature distribution at lying position for $Ra_L=3.795\times10^4$, $Pr=0.707$, $a=20$ mm, $\varepsilon_i=0.688$, $\varepsilon_o=0.400$.

△: $v=\pi/2$ ⊙: $v=\pi/3$
▽: $v=\pi/6$ ●: $v=0$
□: $v=-\pi/6$ ○: $v=-\pi/3$
◇: $v=-\pi/2$ —: numerical

3.3. Comparison of Experimal and Numerical Results

Among the experiments performed, one result with $Ra_L=3.08\times10^4$ for the largest gap ratio, G=0.456, was chosen for comparison, since the appearence of temperature inversion indicated the separation of the inner and outer cylinder thermal boundary layers, and the flow belonged to the two-dimensional laminar boundary layer region which made the application of theoretical approch possible. The agreement of this comparison indicates that the theoretical study can be validly applied to a case which is less influenced by convective flow than this.

Fig. 12 shows the comparison between numerical and experimental result at laying posion. In interferogram the temperature differences between each fringe are 3.15°C and 3.25°C near inner and outer cylinder respectively, while in the numerical result, the difference is 0.1 in dimensionless temperature which corresponds to 2.78°C of experimental result.

Quantitative comparisons of the temperature

distributions at lying position is shown in Fig. 13. Good agreements are attained. Particularly since the fringes are more narrow in the boundary layers adjacent to each cylinder, the agreement is more accurate than in the rest portion of the annulus.

There are errors in the experimental result from end effect, imperfect infinite fringe adjustment of the interferometer and imperfect isothermal conditions in elliptic cylinders. The errors in numerical result arise from Boussinesq approximation, the finite number of nodes and the convergence level of the solutions. Though it is not perfect due to the errors mentioned above, the agreement, which shows the validity of both experimental and theoretical methods, is fairly good.

4. Conclusion

The results of a numerical and experimental investigation for natural convection in annuli between two horizontal confocal elliptic cylinders have been presented. By the good agreement between experimental and numerical results, the validity of this method of analysis which is more expansible without much difficult compared with the previous methods has been shown.

In numerical study, the phenomena in elliptic annulus are shown to be much similar to those of circular annulus which were reported by previous investigators when the Rayleigh number is moderately small at the range of test eccentricities, but some particular phonomena are shown in high Rayliegh number.

In expermental study, the eccentricity of outer cylinder was 0.4 and those of inner cylinder were 0.688, 0.574 and 0.474, resulting in the values of G, 0.456, 0.257 and 0.104 respectively. Usually, the flow which could be known by observation of interferograms is more stable at standing position than at lying position. When G is 0.456, the flow adheres to the two-dimensional pattern until $Ra_L = 7.349 \times 10^4$ even if there were some oscillations. But in the case of G=0.257 the flow becomes oscillatory at $Ra_L = 1.805 \times 10^4$ already. For the smallest gap ratio G=0.104, the influence of natural convection hardly appears until the temperature difference ΔT reaches to 92°C. But in the upper portion of annulus, the "hump" pattern is observed in the interferograms which indicate the appearence of counter-rotating-flow, at relatively high temperature difference. At the similar range of Ra_L, as decreasing gap ratio, the convective motion weakens and flow pattern becomes unstable at first and becomes stable again.

References

1. T.H. Kuehn, Natural convection heat transfer from a horizontal circular cylinder to a surrounding cylindrical enclosure, Ph. D. thesis, University of Minnesota (1976)
2. T.H. Kuehn and R.J. Goldstein, An experimental and theoretical study of natural convection in the annulus between horizontal concentric cylinders, *J. Fluid Mechanics*, 74, 695-719 (1976)
3. E.H. Bishop, C.T. Carley and R.E. Powe, Natural convective oscillatory flow in cylindrical annuli, *Int. J. Heat Mass Transfer*, 11, 1741-1752 (1968)
4. J.H. Lee, A study of natural convection in the annuli between two horizontal elliptic cylinders, Ph. D. thesis, Seoul National University (1979)